Adaptive State Feedback Control Method Based on Recursive Least Squares

Mehmet Latif Levent[1, *], Omer Aydogdu[2]
[1]*Department of Electrical and Electronics Engineering, Faculty of Engineering, Hakkari University, 30000 Hakkari, Turkey*
[2]*Department of Electrical and Electronics Engineering, Faculty of Engineering and Natural Sciences, Konya Technical University, 42250 Selcuklu, Konya, Turkey*
mehmetlatiflevent@hakkari.edu.tr

***Abstract*—This study revealed an adaptive state feedback control method based on recursive least squares (RLS) that is introduced for a time-varying system to work with high efficiency. Firstly, a system identification block was created that gives the mathematical model of the time-varying system using the input/output data packets of the controller system. Thanks to this block, the system is constantly monitored to update the parameters of the system, which change over time. Linear quadratic regulator (LQR) is renewed according to these updated parameters, and self-adjustment of the system is provided according to the changed system parameters. The Matlab/Simulink state-space model of the variable loaded servo (VLS) system module was obtained for the simulation experiments in this study; then the system was controlled. Moreover, experiments were carried out on the servo control experimental equipment of the virtual simulation laboratories (VSIMLABS). The effectiveness of the proposed new method was observed taking the performance indexes as a reference to obtain the results of the practical application of the proposed method. Regarding the analysis of simulation and experimental results, the proposed approach minimizes the load effect and noise and the system works at high efficiency.**

***Index Terms*—Adaptive state feedback; LQR; Recursive least squares; System identification; Variable loaded servo.**

I. INTRODUCTION

Adaptive control is defined as controller structures that can change their behavior against disturbance effects such as system uncertainties, variable load, and noise. Adaptive controllers, in principle, are used to improve functionality and performance. Adjustable parameters and adaptation mechanisms depending on situations are designed in such systems. There are many adaptive controller structures in literature such as model reference adaptive control, adaptive control with state feedback, self-adjusting regulator, and real-time parameter estimation-based adaptive control. Moreover, there are also the following adaptive control applications: stabilization of the terminal voltage of the photovoltaic generator [1], permanent magnet synchronous motor speed control [2], asynchronous motor drive control [3], cruise control system [4], tractor-trailer mobile robot control [5], control of space vehicles [6].

Manuscript received 26 February, 2022; accepted 11 May, 2022.

Approaches that are used as system identification methods, such as Kalman filter, model type converter, particle filter, extended Kalman filter, unscented Kalman filter, iterative polynomial model estimator, and recursive least squares (RLS) estimator, are also encountered in adaptive control systems. Moreover, appropriate modeling for the system is carried out using algorithms such as the linear identified model, nonlinear grey-box model, nonlinear ARX model, and Hammerstein-Wiener model. Hybrid adaptive position controller design in which RLS estimator, disturbance observer and Lyapunov methods are used together [7], RLS estimator method based on a discrete-time sliding mode controller used in the control of the DC motor speed [8], and the RLS approach, which estimates the parameters of the DC motor model [9], can be given as examples to adaptive controller designs. Adaptive designs developed are also tested on other systems. There are studies in which the values of the system parameters are estimated using the RLS method and high performance control [10] is performed to ensure stable operation of a one-wheeled robot. A study carried out on a robotic manipulator proposed an adaptive approach using the Kalman filter (KF) to estimate the linear acceleration and angular velocities of the load and the RLS method to define the load parameters [11]. RLS-based adaptive methods are also used in electric vehicles that have become the focus of researchers in recent years. Approaches such as the iterative least squares method with adaptive forgetting factor [12], the RLS adaptive extended Kalman filter algorithm [13], and the adaptive heuristic critical based RLS algorithm [14] are preferred in system identification and controller designs for lithium-ion batteries, which are a very important part of electric vehicles, to operate at high performance.

The linear quadratic regulator (LQR) method, known as linear optimal state feedback control and is used in adaptive control mechanisms, aims to minimize the errors that occur in the state output values. LQR is a method that increases system performance and stability [15]. The most suitable control input is produced by using the controller gain coefficients calculated with LQR. Thus, a response curve close to the desired reference value can be obtained. LQR control in state feedback servo control systems is used

together with the Kalman filter, which estimates the real states of the system, especially in noisy environments [16], [17]. This study estimated LQR parameters with the RLS-based system identification block.

In this paper, first Section II discusses the discrete-time state-space model of the VLS system. Section III gives a discrete-time LQR model, in which the state feedback matrix calculation is made. Section IV presents the parameter estimation approach with the RLS method. Section V includes an adaptive state feedback control method-based RLS. Finally, the simulation and experimental results are discussed in Section VI.

II. DISCRETE-TIME STATE-SPACE MODEL OF THE VLS SYSTEM

In the beginning, the transfer function of the system should be computed to obtain the discrete-time state-space model of the VLS system. The reduced transfer function of the system (L_m, negligible) is obtained as follows considering the motor and load parameters in Table I.

TABLE I. BRUSHED DC MOTOR AND VLS SYSTEM PARAMETERS.

Symbol	Definition	Value
R_m	Motor armature resistance	2.9 Ω
L_m	Motor armature inductance	0.278 mH
k_t	Motor torque constant	0.0256 Nm/A
k_m	Motor back-EMF constant	0.0256 V/(rad/s)
J_m	Motor inertia	1.49×10^{-6} kgm^2
J_D	Disk inertia	2.125×10^{-5} kgm^2
J_l	Load inertia	1.75×10^{-5} kgm^2
B_m	Motor viscous coefficient	≅ (negligible)
B_l	Load viscous coefficient	0.989×10^{-4} Nms
Initial Load		
J_s	Initial load inertia	2.274×10^{-5} kgm^2
B_s	Initial viscous coefficient	3.544×10^{-6} Nms
Variable Load		
J_{eq}	Load inertia	$\begin{cases}2.274\times10^{-5}\ \text{kgm}^2, 0<t<t_1\\ 3.024\times10^{-5}\ \text{kgm}^2, t_1\le t\end{cases}$
B_{eq}	Load viscous coefficient	$\begin{cases}3.544\times10^{-6}\ \text{Nms}, 0<t<t_1\\ 1.024\times10^{-4}\ \text{Nms}, t_1\le t\end{cases}$

The discrete-time transfer function of the VLS system is obtained by using the expression of the transfer function "$s=e^{-\tau s}\ \left(\tau=kT_s+\rho \text{ ve } 0\le\rho<T_s\right)$" transformation obtained in (1) (with the zero order hold (ZOH) method for the second sampling period $T_s=0.001$) as follows

$$G(s)=\frac{Y(s)}{U(s)}=\frac{0.0256}{5.834\times10^{-9}s^2+6.086\times10^{-5}s+0.00067}. \quad (1)$$

The discrete-time model given by (2) can be written as (3) in the controllable canonical form:

$$G(z)=\frac{Y(z)}{U(z)}=\frac{0.3788z^{-1}+0.03999z^{-2}}{1-0.989z^{-1}+2.947\times10^{-5}z^{-2}}, \quad (2)$$

$$Y(z)=-z^{-1}\left(-0.989Y(z)-0.3788U(z)\right)-$$
$$-z^{-2}\left(2.947e-05Y(z)-0.03999U(z)\right). \quad (3)$$

Discrete-time state-space expressions of the VLS system:

$$x\left[(k+1)T\right]=Ax\left[kT\right]+Bu\left[kT\right], \quad (4)$$

$$y\left[kT\right]=Cx\left[kT\right]+Du\left[kT\right]. \quad (5)$$

In state-space form,

$$x\left[kT\right]=\begin{bmatrix}x_1\left[kT\right]\\ x_2\left[kT\right]\\ x_3\left[kT\right]\end{bmatrix}=\begin{bmatrix}\theta_m\left[kT\right]\\ \omega_m\left[kT\right]\\ i\left[kT\right]\end{bmatrix}. \quad (6)$$

In this case, transformation parameters and state-space matrixes are found as follows: $\beta_0=0$, $\alpha_1=-0.989$, $\beta_1=-0.3788$, $\alpha_2=2.947\times10^{-5}$, $\beta_2=-0.3999$,

$$A=\begin{bmatrix}0 & 0 & 0\\ 1 & 0 & 2.947\times10^{-5}\\ 0 & 1 & 0.989\end{bmatrix},\ B=\begin{bmatrix}0\\ -0.3999\\ -0.3788\end{bmatrix},\ C=\begin{bmatrix}0 & 0 & 1\end{bmatrix},$$

$D=0$.

The matrixes "*A*" and "*B*" are time-invariant matrixes with constant coefficients, as described above, for time-invariant systems. In such systems, optimum control is achieved with constant coefficient controllers such as LQR. However, as the load changes over time, the coefficients of the *A* and *B* matrix change in systems that vary over time. In this situation, it is necessary to constantly update the *A* and *B* matrixes and use the updated *A*, *B* matrixes for optimal control of the VLS system:

$$A=\begin{bmatrix}0 & 0 & 0\\ 1 & 0 & -\alpha_2\\ 0 & 1 & -\alpha_1\end{bmatrix}, \quad (7)$$

$$B=\begin{bmatrix}0\\ \beta_2\\ \beta_1\end{bmatrix}. \quad (8)$$

In this study, the parameter values were constantly observed for changing load. The observable matrix form given above was constantly updated with the RLS method, and thus, the variable load effect is minimized.

III. DISCRETE-TIME LQR MODEL

The LQR technique that is preferred in many control applications is a method that is frequently used in modern optimal control theory and can compute the optimal feedback gain value for stable operation of state feedback systems [18].

Regarding the discrete-time LQR model, the expression that gives the most appropriate control input for the state feedback control method is given by (9) below

$$u[kT] = -K_{lqr} x[kT]. \quad (9)$$

Moreover, the discrete-time quadratic cost function that is used to minimize is also given in (10)

$$J(u) = \sum_{n=1}^{\infty} \begin{pmatrix} x[kT]^T Qx[kT] + u[kT]^T Ru[kT] + \\ +2x[kT]^T Nu[kT] \end{pmatrix}. \quad (10)$$

The equation for a discrete-time system is as follows

$$x[(k+1)T] = Ax[kT] + Bu[kT]. \quad (11)$$

Since "*N*" is a negligible value in the discrete-time quadratic cost function in (10), it can be written *N = 0*. The situation obtained from the discrete-time Riccati equation in (12) is shown in (13) feedback gain matrix:

$$A^T SA - S - (A^T SB)(B^T SB + R)^{-1}(B^T SA) + Q = 0, \quad (12)$$

$$K_{lqr} = (B^T SB + R)^{-1} B^T SA. \quad (13)$$

IV. Parameter Estimation by RLS Method

The least squares method is a standard regression method that is utilized to write the mathematical connection between two physical quantities that vary depending on each other as an equation that is as realistic as possible. In other words, this method is used to find a function curve that will fit "as close as possible" to the measured data points. For the Gauss-Markov theorem, the least squares method is the optimal method for regression.

Recursive least squares (RLS) is an adaptive filter algorithm that iteratively finds the coefficients that minimize the weighted linear least squares cost function by utilizing input data. This approach is different from other algorithms, such as least mean squares (LMS), which aim to reduce the mean square error. The input signals are considered deterministic in deriving RLS while they are considered stochastic for LMS and similar algorithms. RLS converges extremely fast, but it is also a disadvantage that it requires complex and high computation when we compared with most of its competitors.

The RLS estimator uses a general equation expression as given below to estimate the parameters of a linear system. In this equation, $\theta(t)$ values are computed using the known variables $y(t)$ and $H(t)$

$$y(t) = H(t)\theta(t). \quad (14)$$

Recursive algorithms are used for online parameter estimations in calculations. Recursive algorithms are divided into two: infinite history and finite history. Infinite history algorithms calculate from the beginning at all time intervals to minimize the error between observed and predicted outputs. Infinite history algorithms are implemented using RLS estimator and recursive polynomial model estimator blocks in a Matlab/Simulink environment. Finite history algorithms calculate at certain time intervals to minimize the error between observed and predicted outputs. Finite history algorithms are implemented by using RLS estimator and recursive polynomial model estimator blocks in Matlab/Simulink environment. Regarding the comparison of infinite history algorithms, parameter estimations can be made more easily with finite history algorithms in situations where parameter values change quickly and abruptly. Equation (15) shows the general expression of the infinite past iterative estimation algorithm

$$\hat{\theta}(t) = \hat{\theta}(t-1) + K(t)(y(t) - \hat{y}(t)), \quad (15)$$

where $\hat{\theta}(t)$ are the parameters predicted at moment of "*t*" while $y(t)$ is the output signal observed at the moment of "*t*" and $\hat{y}(t)$ is the instantaneously observed signal at time *(t - 1)* of $y(t)$. Gain value ($K(t)$) determines how much the current estimation error ($y(t) - \hat{y}(t)$) will affect the update of the parameter estimation. In general, recursive prediction algorithms minimize the expression of the estimation error ($y(t) - \hat{y}(t)$). The gain expression $K(t)$ is written by the equation below

$$K(t) = Q(t)\psi(t), \quad (16)$$

where $Q(t)$ is the minimized function, $\psi(t)$ is defined as the gradient of the estimated model output ($\hat{y}(t|\theta)$). The recursive algorithms supported by the Matlab System identification toolbar vary based on different approaches consisting of different calculations in $Q(t)$ and $\psi(t)$ values. The expression of parameter gradient is shown with the linear regression equation in (17)

$$y(t) = \psi^T(t)\theta_0(t) + e(t). \quad (17)$$

In this expression, $\psi(t)$ is the regression vector that is computed based on input-output values measured in the previous iteration. $\theta_0(t)$ is the values of the real parameters. The noise source that is accepted as white noise is expressed with $e(t)$. Estimated output equation is given below. The infinite history recursive prediction algorithms used for online control of the system are divided into three categories, including forgetting factor, Kalman filter, and gradient

$$\hat{y}(t) = \psi^T(t)\hat{\theta}(t-1). \quad (18)$$

The formulas for the forgetting factor and the Kalman algorithm are more complex compared to the formulas used in the gradient method. However, it typically displays a better convergence feature. This study used the Kalman filter and obtained simulation and experimental results. Kalman filter equations that are used as a model fitting algorithm are given below. R_1 is the parameter change

covariance matrix that is determined by the user. Moreover, $R_2 \times P$ is the covariance matrix of estimated parameters, while R_1 / R_2 is the parameter change covariance matrix:

$$\hat{\theta}(t) = \hat{\theta}(t-1) + K(t)\left(y(t) - \hat{y}(t)\right), \tag{19}$$

$$\hat{y}(t) = \psi^T(t)\hat{\theta}(t-1), \tag{20}$$

$$K(t) = Q(t)\psi(t), \tag{21}$$

$$Q(t) = \frac{P(t-1)}{R_2 + \psi^T(t)P(t-1)\psi(t)}, \tag{22}$$

$$P(t) = P(t-1) + R_1 - \frac{P(t-1)\psi(t)\psi(t)^T P(t-1)}{R_2 + \psi(t)^T P(t-1)\psi(t)}. \tag{23}$$

The expression in (23) can be defined in linear regression form by the equation below

$$y(t) = \psi^T(t)\theta_0(t) + e(t). \tag{24}$$

$Q(t)$ value in (22) is computed with the Kalman filter. The expression $\theta_0(t)$ that is the real parameter is calculated as follows

$$\theta_0(t) = \theta_0(t-1) + w(t), \tag{25}$$

where $w(t)$ is known as Gaussian white noise. The relation between $w(t)$ and parameter change covariance matrix R_1 is shown by the equation below

$$Ew(t)w^T(t) = R_1. \tag{26}$$

The values R_2 above equals the variance of the value $e(t)$. The expression $e(t)$ is written as follows if there is $y(t) = \psi^{T(t)}\theta_0(t) + e(t)$

$$e(t) = y(t) - \psi^T(t)\theta_0(t). \tag{27}$$

Finally, Kalman filter algorithms are specified by recording output signal $y(t)$, gradient R_1, R_2 values with the first estimated values of parameters and $P(t=0)$ values (covariance matrix including parameter errors) to the system. Moreover, R_1 and $P(t=0)$ matrixes are accepted as scaled values such as $R_2 = 1$. Regarding scaling, it does not affect parameter estimation.

V. RLS-BASED ADAPTIVE STATE FEEDBACK CONTROL

This chapter discusses the recursive least squares (RLS) method and the system identification-based adaptive state feedback control method. This proposed approach consists of three main parts: system identification, parameter estimation, and state feedback. Figure 1 shows the block diagram of the adaptive state feedback control system. As is seen in figure, the mathematical model is obtained by using the input/output data of the VLS system, which is controlled by the system identification block In this block, the system output for each input is monitored online, with system identification model fitting algorithms. Optimum K_{lqr} values are specified on the basis of matrixes *A*, *B*, and *C* that are obtained for the initial load of the controlled VLS system to make the system work as state feedback. Moreover, RLS system identification block running in the background is also added to the system. The RLS method is a good learning technique and it also gives desired results with updated parameter values compared to the previous iteration. For this reason, it is impossible to receive the desired response in the first iteration. However, it is possible to obtain the real model of the system in a process of time. The system identification block occurs in three stages.

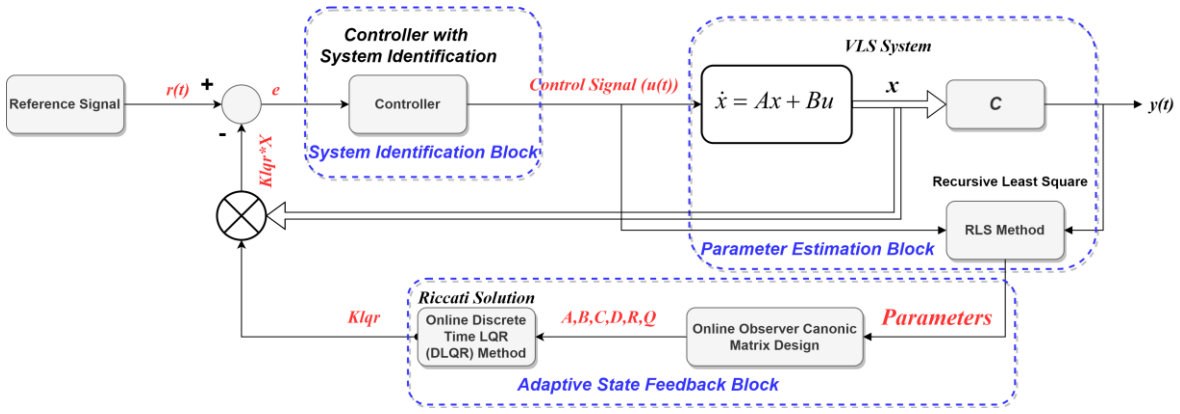

Fig. 1. RLS-based adaptive state feedback control block diagram.

During the period determined in the first stage, open-loop input/output data packets are saved at the initial load of the controlled system. In the second stage, these saved data are defined in the system identification method for use. Finally, the transfer function of the controller providing the most appropriate response curve is obtained by applying different model fitting algorithms. Figure 2 shows the experimental operating principle of the system identification process. Parameter estimation is performed using the system output and control input data in the adaptive state feedback control structure. As the operation of the system continues, the parameter values are constantly updated. The necessary parameter data are provided for the online calculation of the observable canonical form matrix values of *A*, *B*, *C*, *R*, and *Q* via the parameter estimation block. Finally, as is seen in Fig. 3, matrix values are defined as inputs of the online

LQR control block. The optimal K_{lqr} value is calculated online after the calculation of the Riccati equation is performed.

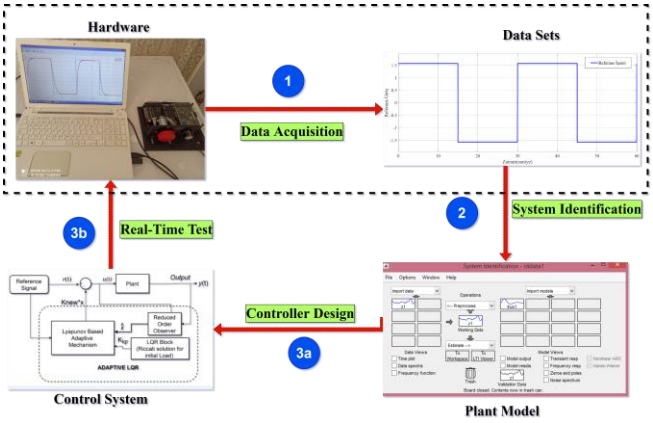

Fig. 2. Work principle of system identification.

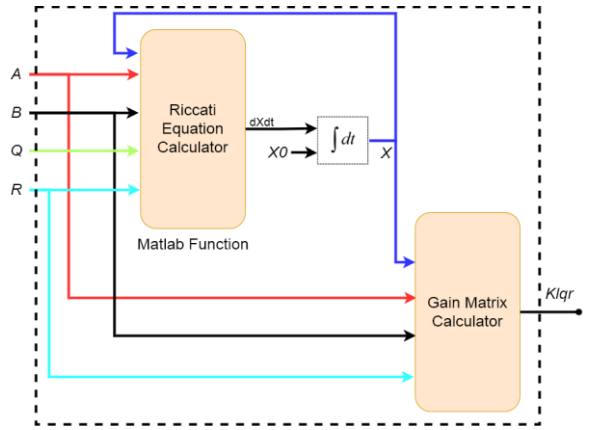

Fig. 3. Online discrete-time LQR control.

VI. Simulation and Experimental Results

The position or trajectory control of the VLS system is simulated and applied by using the RLS-based adaptive state feedback control method in this chapter. Figure 4 shows the experimental set of the servo system used in the application study.

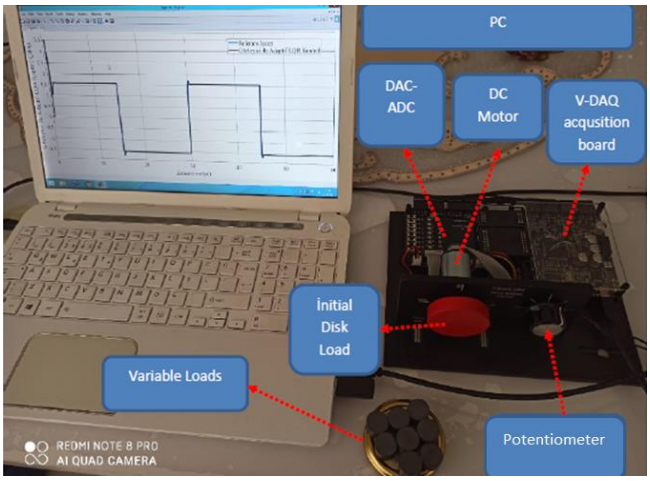

Fig. 4. Servo control experimental equipment of virtual simulation laboratories (VSIMLABS).

This set includes a laptop, DC Motor, disc-shaped variable load, potentiometer, DAC-ADC board and V-DAQ board. With the VSIMLABS system, various control experiments can be performed with high performance and accuracy in the Matlab/Simulink environment.

A. Simulation Results

In this chapter the system identification toolbar in the Matlab environment is used to provide an optimal control signal for a time-invariant servo system. The input/output data packets of the open-loop system are identified in the interface of this toolbar in a suitable format. For this purpose, a random reference signal was applied to the open-loop servo system and the obtained input-output data were saved in Matlab workspace to be used in the system identification toolbar. Then, system identification model fitting algorithms such as Gauss-Newton, Adaptive Gauss-Newton, Interior-Point, and Levenberg-Marquardt were applied to obtain the optimal response curve.

Table II shows the performance percentages of first order, second order, and third order system transfer functions and response curves using the system identification toolbar. The transfer functions estimated here are used in the controller design. The Gauss-Newton and Levenberg-Marquardt algorithms give the best performance with a success rate of 91.4 % when the transfer functions estimated for the second order system are applied to the system. Figures 5 and 6 give the results of the second order system identification. Regarding the zoomed response curve, the lowest error value between the reference signal and the output curves was obtained by the Levenberg-Marquardt and Gauss-Newton algorithms.

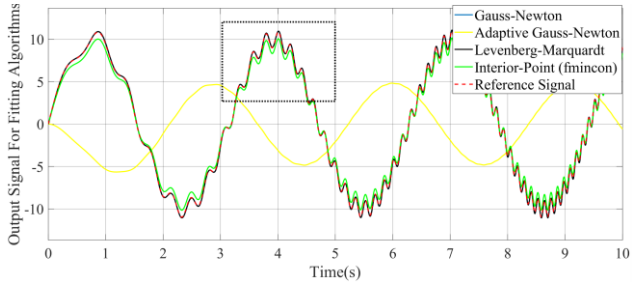

Fig. 5. Simulation results of system identification model fitting algorithms (second order).

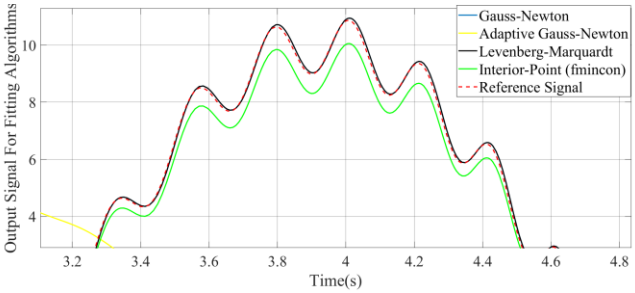

Fig. 6. Zoom area for Fig. 5.

On the other hand, the desired results were not obtained when the data packages of the system were used in the Adaptive Gauss-Newton method.

B. Experimental Results

This chapter discusses trials of the VSIMLABS servo control equipment.

TABLE II. PERFORMANCE PERCENTAGES OF RESPONSE CURVES OBTAINED BY SYSTEM IDENTIFICATION ALGORITHMS (1D: FIRST ORDER, 2D: SECOND ORDER, 3D: THIRD ORDER).

	Transfer Function			Performance Percentages		
	First Order	**Second Order**	**Third Order**	**1D**	**2D**	**3D**
G.-Newton	$\frac{236.1}{s+232.2}$	$\frac{-9013}{s^2+7852s+9571}$	$\frac{3.804\times10^6}{s^3+328.1s^2+4.371\times10^4 s+3.796\times10^6}$	84.3	91.4	84.6
A. G.-Newton	$\frac{2.041\times10^5}{s+2.049\times10^5}$	$\frac{4.567\times10^4}{s^2+155.2s+4.54\times10^4}$	$\frac{3.804\times10^6}{s^3+419.1s^2+2.45\times10^4 s+3.796\times10^6}$	89.3	-0.1	80.1
Interior-Point	$\frac{2.436\times10^5}{s+2.451\times10^5}$	$\frac{1.007\times10^5}{s^2+147.5s+1.089\times10^5}$	$\frac{3.804\times10^6}{s^3+338.3s^2+2.664\times10^4 s+3.796\times10^6}$	81.7	85.5	84.4
L.-Marquardt	$\frac{3.001\times10^8}{s+3.013\times10^8}$	$\frac{4.567\times10^4}{s^2+155.2s+4.54\times10^4}$	$\frac{1.091\times10^7}{s^3+586.2s^2+9.402\times10^4 s+1.101\times10^7}$	84.3	91.4	85.4

Figures 7 and 8 show the application results obtained when using the RLS Kalman filter algorithm for the RLS-based adaptive control method in a constant load environment. Regarding the output curves of the system, the maximum performance of the system is obtained for the value of R1 = 0.3. According to these results, the applied control method learned the system as the iterations progressed.

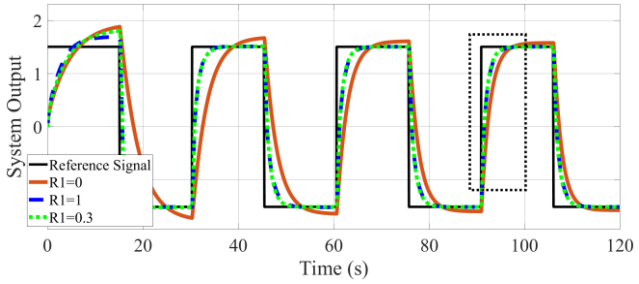

Fig. 7. Kalman filter system output for the initial load condition.

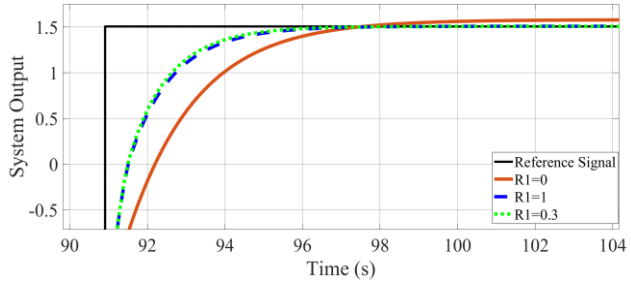

Fig. 8. Zoom area for Fig. 7.

Figures 9 and 10 show the change curves in the parameters obtained by the feedback gain matrix value and the recursive least squareslow method. For the findings, the estimated parameter values are constantly updated, and the system output produces good results in parallel. Then, the results that were obtained when the variable load effect is added to the system after the 100th second are given.

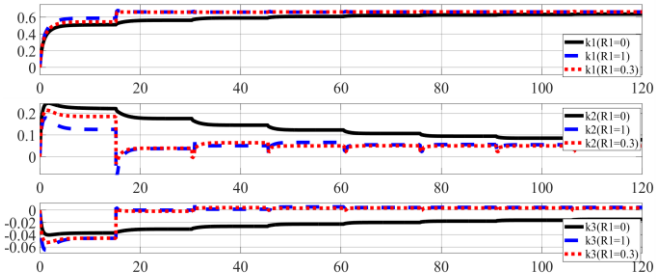

Fig. 9. Change of gain matrix value.

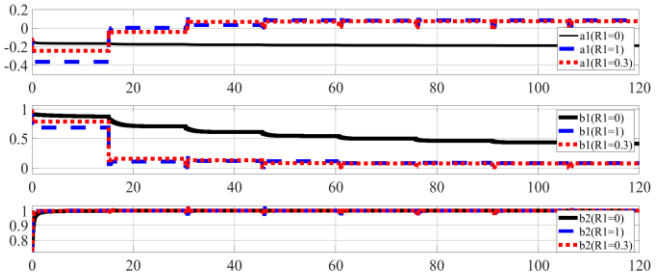

Fig. 10. Change of system parameters for the initial load condition.

The response in Fig. 11 shows that the load that affects the system with the designed controller is minimized. Regarding the expanded response curve in Fig. 12, although there are high-amplitude oscillations for the gain value R1 = 0.3, it does not affect the system performance after the load effect.

On the other hand, maximum system performance was obtained for the value of R1 = 0.3. The load effect was quickly compensated with this proposed method; the output signal settled on the reference signal with low-amplitude oscillation. Figures 13 and 14 show the change in feedback gain matrix value K_{lqr} and parameters that were estimated

by the RLS method, respectively.

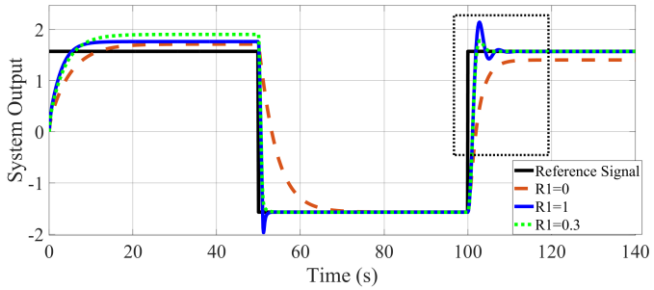

Fig. 11. Kalman filter output responses (load added at 100 seconds).

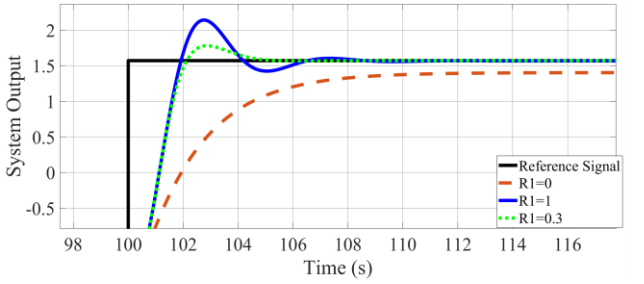

Fig. 12. Zoom area for Fig. 11.

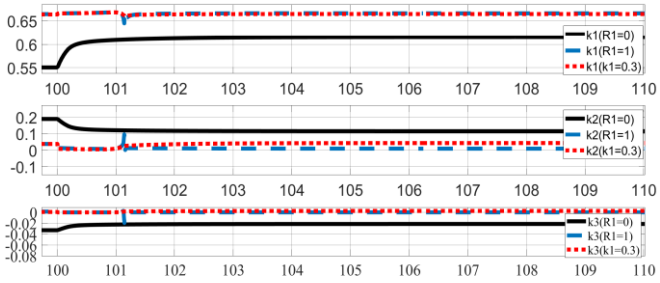

Fig. 13. Change of gain matrix value for variable load after 100th second.

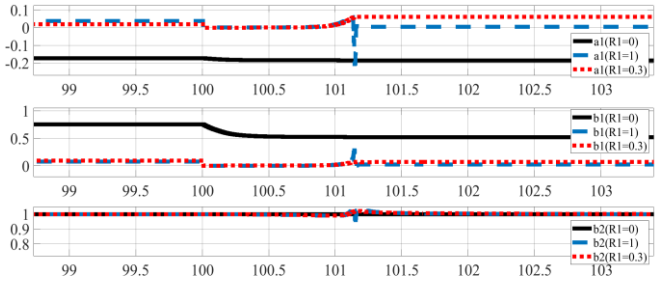

Fig. 14. Change of system parameters for variable load after 100th second.

The results obtained using the RLS Kalman filter algorithm in this study are given above. Also, forgetting factor algorithm is used for the VLS system, and the results are given in Figures 15 and 16. According to the reference index given in Table III, it was concluded that the proposed method produced the desired results.

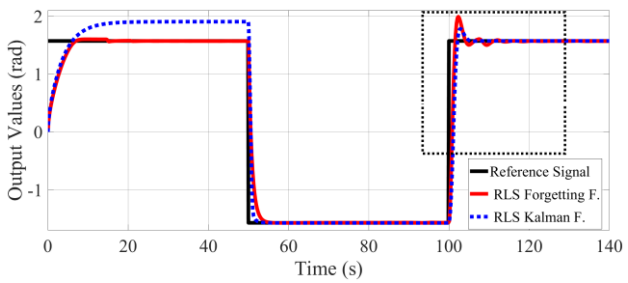

Fig. 15. Result of RLS Kalman filter and RLS forgetting factor.

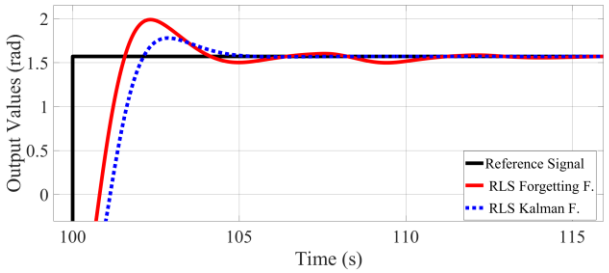

Fig. 16. Zoom area for Fig. 15 (after 100th second).

TABLE III. VLS SYSTEM PERFORMANCE INDEX RESULTS (*ISE*: INTEGRAL SQUARE ERROR, *IAE*: INTEGRAL ABSOLUTE ERROR, *ITAE*: INTEGRAL TIME ABSOLUTE ERROR).

Method	ISE	IAE	ITAE
RLS Kalman filter	3.240	2.214	61.94
RLS forgetting factor	3.548	2.343	57.89

In the previous study [19], the LQR method was applied to the same system with the discrete-time Kalman filter. However, when the transient response analysis was performed for this system, multiple oscillations and amplitudes with high values occurred. The oscillations and high amplitudes in this system are compensated by the proposed method.

VII. CONCLUSIONS

First, the parameter estimations of the system were performed by the least squares method in the state feedback control design using the least squares method. Online discrete-time *A*, *B*, *C*, *D*, *R*, and *Q* matrix calculations were made with these parameters. Thus, the optimal K_{lqr} value was calculated and a high-performance controller was designed via the updated system matrix values online. A high-performance controller design was carried out. Moreover, an RLS system identification block running in the background is also added to the system. The RLS method is a good learning technique and it also gives desired results with updated parameter values compared to the previous iteration. For this reason, it is impossible to receive the desired response in the first iteration. Block initial conditions in the system identification block are defined taking into account the known constant load VLS system parameters to quickly solve this problem. Thus, the performance is improved. It is observed that it works under the desired criteria when the RLS-based state feedback control method is applied to the system. According to the results, disruptive effects such as variable load and noise in the system are minimized and the system is ensured to operate at high efficiency. In the adaptive state feedback control system designed using the least squares method, the forgetting factor or Kalman filter value is entered manually, and the optimum value is found by observing the results. An adaptation mechanism that enables this value to be updated online is important for system performance. Future works aim to solve this problem.

CONFLICTS OF INTEREST

The authors declare that they have no conflicts of interest.

REFERENCES

[1] Y. Malinkovich, S. Lineykin, and M. Sitbon, "Analysis, modeling, and simulation of adaptive control based on dynamic conductance estimation of photovoltaic generator interfaced current-mode buck converter", *Elektronika ir Elektrotechnika*, vol. 28, no. 1, pp. 32–41, 2022. DOI: 10.5755/j02.eie.29205.

[2] R. Szczepanski, T. Tarczewski, and L. M. Grzesiak, "PMSM drive with adaptive state feedback speed controller", *Bulletin of the Polish Academy of Sciences: Technical Sciences*, vol. 68, no. 5, pp. 1009–1017, 2020. DOI: 10.24425/bpasts.2020.134624.

[3] A. Devanshu, M. Singh, and N. Kumar, "Adaptive predictive current control of field-oriented controlled induction motor drive", *IETE Journal of Research*, pp. 1–13, 2020. DOI: 10.1080/03772063.2020.1775502.

[4] A. Abdullahi and S. Akkaya, "Adaptive cruise control: A model reference adaptive control approach", in *Proc. of 2020 24th International Conference on System Theory, Control and Computing (ICSTCC)*, 2020, pp. 904–908. DOI: 10.1109/ICSTCC50638.2020.9259641.

[5] O. Elhaki and K. Shojaei, "Observer-based neural adaptive control of a platoon of autonomous tractor–trailer vehicles with uncertain dynamics", *IET Control Theory & Applications*, vol. 14, no. 14, pp. 1898–1911, 2020. DOI: 10.1049/iet-cta.2019.1403.

[6] S. Xiang and S. Fang, "DSMC study for effects of angles of attack on closed cavity of space vehicle in hypersonic rarefied flow", in *Aerospace Mechatronics and Control Technology. Springer Aerospace Technology*. Springer, Singapore, 2022, pp. 43–56. DOI: 10.1007/978-981-16-6640-7_4.

[7] D. Ruan, H. Xie, K. Song, and G. Zhang, "Adaptive speed control based on disturbance compensation for engine-dynamometer system", *IFAC-PapersOnLine*, vol. 52, no. 5, pp. 642–647, 2019. DOI: 10.1016/j.ifacol.2019.09.102.

[8] J. D. Valladolid, J. P. Ortiz, and L. I. Minchala, "Adaptive quasi-sliding mode control based on a recursive weighted least square estimator for a DC motor", in *Proc. of 2016 IEEE Conference on Control Applications (CCA)*, 2016, pp. 886–890. DOI: 10.1109/CCA.2016.7587925.

[9] J. Jimenez-Gonzalez, F. Gonzalez-Montañez, V. M. Jimenez-Mondragon, J. U. Liceaga-Castro, R. Escarela-Perez, and J. C. Olivares-Galvan, "Parameter identification of BLDC motor using electromechanical tests and recursive least-squares algorithm: Experimental validation", *Actuators*, vol. 10, no. 7, p. 143, 2021. DOI: 10.3390/act10070143.

[10] S. Farsoni, C. Talignani Landi, F. Ferraguti, C. Secchi, and M. Bonfè, "Real-time identification of robot payload using a multirate quaternion-based kalman filter and recursive total least-squares", in *Proc. of 2018 IEEE International Conference on Robotics and Automation (ICRA)*, 2018, pp. 2103–2109. DOI: 10.1109/ICRA.2018.8461167.

[11] X. Sun, J. Ji, B. Ren, C. Xie, and D. Yan, "Adaptive forgetting factor recursive least square algorithm for online identification of equivalent circuit model parameters of a lithium-ion battery", *Energies*, vol. 12, no. 12, p. 2242, 2019. DOI: 10.3390/en12122242.

[12] Z. Zhou, B. Duan, Y. Kang, N. Cui, Y. Shang, and C. Zhang, "A low-complexity state of charge estimation method for series-connected lithium-ion battery pack used in electric vehicles", *Journal of Power Sources*, vol. 441, art. 226972, 2019. DOI: 10.1016/j.jpowsour.2019.226972.

[13] V. Moghaddam, A. Yazdani, H. Wang, D. Parlevliet, and F. Shahnia, "An online reinforcement learning approach for dynamic pricing of electric vehicle charging stations", *IEEE Access*, vol. 8, pp. 130305–130313, 2020. DOI: 10.1109/ACCESS.2020.3009419.

[14] H. H. Bilgiç, M. A. Şen, M. Kalyoncu, and A. Yapici, "Doğrusal ters sarkacın denge kontrolü için yapay Sinir Ağı Tabanlı Bulanık Mantık & LQR kontrolcü tasarımı", in *Proc. of Otomatik Kontrol Ulusal Toplantısı–(TOK 2014)(Poster)*, Otomatik Kontrol Ulusal Toplantısı Bildiriler Kitabı, 2014, pp. 921–926. DOI: 10.13140/RG.2.1.4983.7204.

[15] A. S. Elkhatem and S. N. Engin, "Robust LQR and LQR-PI control strategies based on adaptive weighting matrix selection for a UAV position and attitude tracking control", *Alexandria Engineering Journal*, vol. 61, no. 8, pp. 6275–6292, 2022. DOI: 10.1016/j.aej.2021.11.057.

[16] Y. Zhi, G. Li, Q. Song, K. Yu, and J. Zhang, "Flight control law of unmanned aerial vehicles based on robust servo linear quadratic regulator and Kalman filtering", *International Journal of Advanced Robotic Systems*, vol. 14, no. 1, pp. 1–7, 2017. DOI: 10.1177/1729881416686952.

[17] H. Maghfiroh, M. Nizam, M. Anwar, and A. Ma'Arif, "Improved LQR control using PSO optimization and Kalman filter estimator", *IEEE Access*, vol. 10, pp. 18330–18337, 2022. DOI: 10.1109/ACCESS.2022.3149951.

[18] C.-C. Chen and Y.-T. Chen, "Feedback linearized optimal control design for quadrotor with multi-performances", *IEEE Access*, vol. 9, pp. 26674–26695, 2021. DOI: 10.1109/ACCESS.2021.3057378.

[19] M. L. Levent, Ö. Aydoğdu, and C. Yücelbaş, "Discrete time state estimation with Kalman filter and adaptive LQR control of a time varying linear system", *European Journal of Science and Technology*, special issue, pp. 322–331, 2020. DOI: 10.31590/ejosat.804741.